Contribution from the Department of Chemistry and Biochemistry, University of California, Los Angeles, California 90024

Luminescence and Absorption Spectroscopy of $Re(O)I(RC{\equiv}CR)_2$ and $[Re(O)PPh_3(RC{\equiv}CR)_2]SbF_6$ ($R = CH_3, C_6H_5$)

Christian Reber and Jeffrey I. Zink*

Received August 15, 1990

Low-temperature luminescence and polarized single-crystal absorption spectra of $Re(O)I(RC{\equiv}CR)_2$ ($R = CH_3, C_6H_5$) and $[Re(O)PPh_3(CH_3C{\equiv}CCH_3)_2]SbF_6$ are presented and interpreted. The title compounds show broad, unstructured luminescence with band maxima near 15000 cm^{-1} (20 K). The luminescence lifetimes at 20 K are $\approx$10 μs for all three compounds. The absorption spectra contain three bands at about 19000, 24000, and 28000 cm^{-1}. They are assigned as d-d transitions based on their intensity. The relative polarizations of the bands together with resonance Raman spectra and molecular orbital calculations are used to support the assignments.

Introduction

Recently a novel class of organometallic rhenium-oxo compounds has been synthesized.[1-3] These compounds contain unusually short rhenium-oxygen bonds on the order of 1.7 Å,[1] two substituted acetylene ligands, and iodide or triphenylphosphine as the fourth ligand. The formal oxidation state of the rhenium ion is +3 and the electron configuration at the metal center is therefore [Xe]$5d^4$. Rhenium is well-known to show a rich organometallic chemistry in high oxidation states.[4]

The rhenium-oxo compounds are very attractive systems for studies of excited electronic states for two reasons. First, only a few coordination compounds with the d^4 electron configuration have been investigated with optical spectroscopic techniques.[5-9] Second, the very short Re-O bond and the correspondingly strong interaction in the title compounds provide a strong ligand field, and luminescence in the visible spectral range is observed. Usually no luminescence is observed from d^4 metal centers due to efficient radiationless relaxation to low-energy ligand field states in the infrared spectral region. The unusually high energy of the emitting state makes it impossible to predict a priori the nature of the lowest excited states. Both d-d and charge-transfer states can be expected at similar energies. Previous work on the title compounds focused on the synthesis, the structure determinations, and the NMR spectroscopic properties.[1-3]

In this paper, the luminescence of the d^4 Re^{3+} title compounds and the electronic absorption and resonance Raman spectra are reported. The nature of the lowest energy excited states is determined by using optical spectroscopy. The main emphasis is on the low-temperature single-crystal luminescence and polarized absorption spectroscopy. Room-temperature resonance Raman spectra are used to support the assignments of the excited states. The assignments are compared to extended Hückel calculations from the literature.[1]

Experimental Section

The syntheses and crystal structures of the title compounds have been reported by Mayer and co-workers.[1-3] The compounds used in this study were gifts from these authors. Single crystals for absorption spectra were grown between quartz plates from hexane solutions in a refrigerator. Polycrystalline samples were used for the luminescence and Raman measurements.

The instruments used for the luminescence[10] and absorption[11] spectroscopic studies and the luminescence lifetime measurements[12] are described in detail elsewhere. For all of the low-temperature measurements, the samples were cooled in a closed-cycle He cryogenic unit (Air Products Displex). The 457.9-nm line of an Ar^+ laser (Coherent Innova 90) was used as the excitation source for the luminescence spectra. All the emission spectra are corrected for the instrument response. The Raman spectra were obtained by using the 514.5- and 457.9-nm lines of the same laser. The scattered light was dispersed by a 0.85-m double monochromator (Spex 1402) and detected with a cooled photomultiplier (RCA C31034) and a photon-counting system (EG+G 1105). The data acquisition for all of the experiments was controlled by a microcomputer.

Table I. Absorption and Emission Band Maxima

compound	abs max, cm^{-1}	emission max, cm^{-1}	Stokes shift, cm^{-1}
$Re(O)I(CH_3C{\equiv}CCH_3)_2$	19100[a]	15700[a]	3400
	23800[a]		
	28100[a]		
$Re(O)I(C_6H_5C{\equiv}CC_6H_5)_2$	19100[b]	15500[a]	3600
	24500[b]		
	28600[b]		
$[Re(O)P(C_6H_5)_3(CH_3C{\equiv}CCH_3)_2]SbF_6$	18600[b]	14900[a]	3700
	25500[b]		
	28200[b]		

[a] T = 20 K. [b] T = 80 K.

Results

Luminescence Spectra. All of the compounds studied here are luminescent in the visible region of the spectrum at low temperatures. The low-temperature spectra are shown in Figure 1. The band maxima are at 15700 cm^{-1} for $Re(O)I(CH_3C{\equiv}CCH_3)_2$, 15500 cm^{-1} for $Re(O)I(C_6H_5C{\equiv}CC_6H_5)_2$, and 14900 cm^{-1} for $[Re(O)PPh_3(CH_3C{\equiv}CCH_3)_2]SbF_6$. All of the emission spectra contain a broad featureless envelope with no vibronic structure.

Both the luminescence lifetimes and the intensities decrease with increasing temperature as shown in Figure 2. The lifetimes at 20 K are 14.5 μs for $Re(O)I(C_6H_5C{\equiv}CC_6H_5)_2$, 14.0 μs for $Re(O)I(CH_3C{\equiv}CCH_3)_2$, and 8.0 μs for $[Re(O)PPh_3(CH_3C{\equiv}CCH_3)_2]SbF_6$. The luminescence intensities of all of the compounds drop to near the limit of detectability at temperatures of about 150 K.

Absorption Spectra. The absorption spectra of all three compounds consist of three resolved bands in the wavenumber region between 15000 and 30000 cm^{-1}. The band maxima and estimated molar absorptivities are listed in Table I. Single crystal polarized absorption spectra of the $Re(O)I(CH_3C{\equiv}CCH_3)_2$ compound are shown in Figure 3. The spectra were obtained by aligning the polarizer along the two extinction directions of the crystal. Because the orientation of the electric vector along the molecular axes is not known, the spectra only provide information about the relative polarizations of the absorption bands. The lowest energy band has the same intensity in both polarization directions while the two higher energy bands are oppositely polarized. The insert to Figure 3 contains the solution absorption spectrum of $Re(O)I(CH_3C{\equiv}CCH_3)_2$. The band positions and intensities are similar to those in the crystal spectra. The lowest energy band is more

(1) Mayer, J. M.; Thorn, D. L.; Tulip, T. H. *J. Am. Chem. Soc.* **1985**, *107*, 7454.
(2) Mayer, J. M.; Tulip, T. H.; Calabrese, J. C.; Valencia, E. *J. Am. Chem. Soc.* **1987**, *109*, 157.
(3) Manion, A. B.; Erikson, T. K. G.; Spaltenstein, E.; Mayer, J. M. *Organometallics* **1989**, *8*, 1871.
(4) Herrmann, W. A. *Angew. Chem., Int. Ed. Engl.* **1988**, *27*, 1297.
(5) Lees, A. J. *Chem. Rev.* **1987**, *87*, 711.
(6) Ferguson, J. *Prog. Inorg. Chem.* **1970**, *12*, 159.
(7) *Concepts of Inorganic Photochemistry*; Adamson, A. W., Fleischauer, P. D., Eds.; Wiley: New York, 1975.
(8) Balzani, V.; Carassiti, V. *Photochemistry of Coordination Compounds*; Academic Press: New York, 1970.
(9) Geoffrey, G. L.; Wrighton, M. S. *Organometallic Photochemistry*; Academic Press: New York: 1979.
(10) Tutt, L. W.; Zink, J. I. *J. Am. Chem. Soc.* **1986**, *108*, 5830.
(11) Chang, T. H.; Zink, J. I. *J. Am. Chem. Soc.* **1984**, *106*, 287.
(12) Larson, L. J.; Zink, J. I. *Inorg. Chem.* **1989**, *28*, 3519.

0020-1669/91/1330-2994$02.50/0

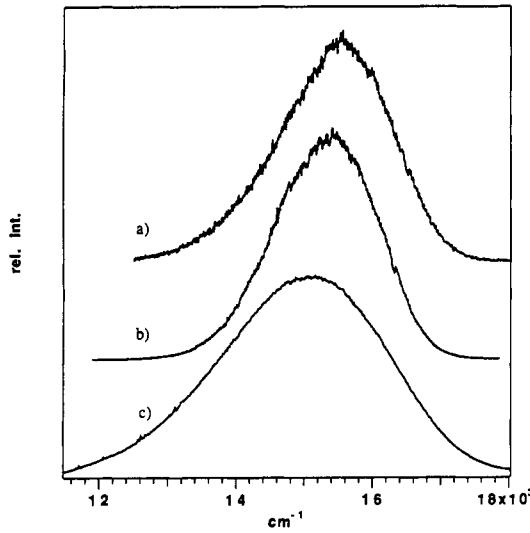

Figure 1. 20 K crystal luminescence spectra of $Re(O)I(C_6H_5C{\equiv}CC_6H_5)_2$ (a), $Re(O)I(CH_3C{\equiv}CCH_3)_2$ (b), and $[Re(O)P(C_6H_5)_3(CH_3C{\equiv}CCH_3)_2]SbF_6$ (c).

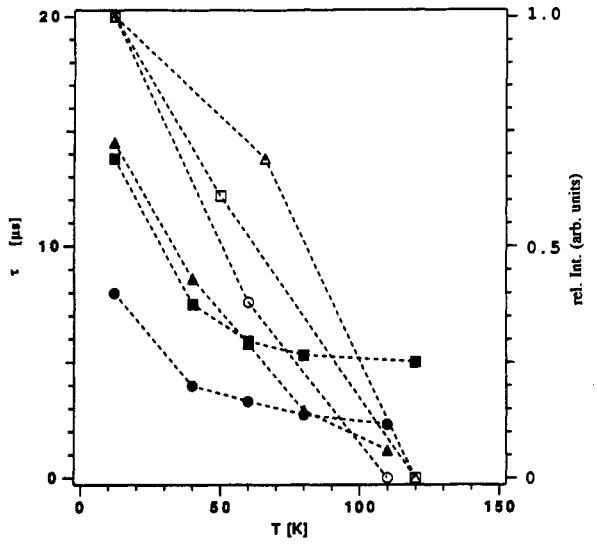

Figure 2. Luminescence lifetimes (full symbols, left-hand ordinate scale) and relative luminescence intensities (open symbols, right-hand ordinate scale) for $Re(O)I(CH_3C{\equiv}CCH_3)_2$ (squares), $Re(O)I(C_6H_5C{\equiv}CC_6H_5)_2$ (triangles) and $[Re(O)P(C_6H_5)_3(CH_3C{\equiv}CCH_3)_2]SbF_6$ (circles).

clearly visible in the solution spectrum due to the better baseline of the solution absorption instrument. The high-energy tail of the emission band overlaps the low-energy tail of the weak, lowest energy absorption band at about 19 000 cm^{-1} in all of the compounds.

Resonance Raman Spectra. Raman spectra with the exciting light in resonance with the lowest energy and the second lowest energy bands were obtained for all three compounds. The wavenumbers of selected bands and their relative intensities are given in Table II. For the relative intensity calculations, the intensities of the C-H modes of the substituted acetylenes were used as internal "standards". In the case of the $Re(O)PPh_3(CH_3C{\equiv}CCH_3)_2^+$ compound, the 649-cm^{-1} mode of the SbF_6^- counterion was used as a check to verify that the intensities of the C-H modes were insensitive to the wavelength of the exciting light. In all of the compounds the Re-O stretching vibration at about 970 cm^{-1} showed pronounced resonance enhancement. The acetylene C≡C stretch showed smaller resonance effects. Intensities were calculated by numerically integrating the experimental spectra.

Discussion

Assignments. The three lowest energy absorption bands and the emission band are assigned to d-d transitions. The primary

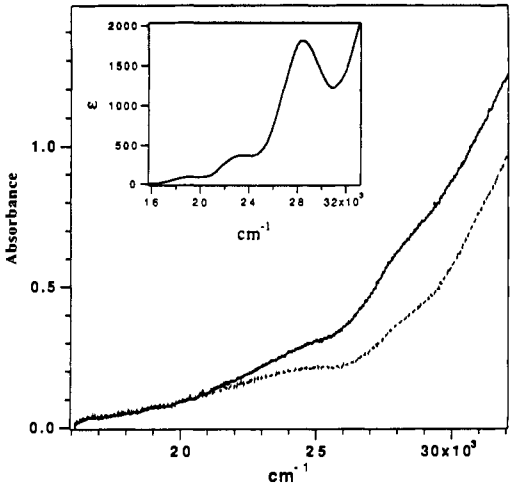

Figure 3. Polarized single-crystal absorption spectra of $Re(O)I(CH_3C{\equiv}CCH_3)_2$ (T = 20 K). The insert shows the absorption spectrum in hexane solution.

Table II. Selected Raman Frequencies and Intensities

compound	energy, cm^{-1}	rel Intens[a]	rel Intens[b]	assignt
$Re(O)I(CH_3C{\equiv}CCH_3)_2$	967	0.67	0.28	Re—O
	1581	0.77	0.70	C≡C
	3085	1	1	C—H
$Re(O)I(C_6H_5C{\equiv}CC_6H_5)_2$	974	0.52	0.20	Re—O
	1600	0.83	0.68	C≡C
	3080	1	1	C—H
$[Re(O)P(C_6H_5)_3(CH_3C{\equiv}CCH_3)_2]SbF_6$	649	0.43	0.50	Sb—F
	971	0.80	0.33	Re—O
	1595	0.93	0.88	C≡C
	3077	1	1	C—H

[a] 514.5-nm excitation. [b] 457.9-nm excitation.

experimental basis for the d-d assignment is the magnitude of the molar absorptivity which is on the order of 10^2-10^3 L/(mol cm) for the three absorption bands (Figure 3). This magnitude is common for "spin-forbidden" d-d transitions in third-row transition-metal complexes.[5] Additional support for this assignment is found in the results of molecular orbital calculations, which show that the complexes can be interpreted in terms of a d^4 rhenium(III) metal center[1] with both the HOMO and LUMO having mainly metal d character. The absorption spectroscopic results are consistent with this assignment as discussed below.

Both the absorption and the luminescence bands are broad, indicative of large structural differences between the final and initial electronic states. This breadth is typical for interconfigurational transitions which have different d-orbital populations of the two states. The overlap of the first absorption and the emission bands indicates that the same excited state is involved in both transitions. It therefore is the lowest energy excited state.

The electronic transitions are interpreted in terms of the d-orbital correlation diagram and the corresponding energy level diagram shown in Figure 4. The starting point for this interpretation is the d-orbital splitting pattern in a tetrahedral field shown on the left of the diagram. The splitting pattern and relative energies in an idealized C_{3v} symmetry calculated by using extended Hückel theory are shown in the second column of Figure 4.[1] In the C_s symmetry of the complexes studied here, the "t_2" and "e" orbitals further split into $a'(d_{z^2}) + a'(d_{xz}) + a''(d_{yz})$ and $a'(d_{x^2-y^2}) + a'(d_{xy})$, respectively, as shown in the third column. The d_{z^2} orbital is strongly σ interacting with the oxo ligand while the d_{xz} and d_{yz} orbitals undergo strong π interactions with the oxo ligand. The d_{z^2} orbital also undergoes strong π interactions with the acetylene ligand. Of specific interest for the following discussion, the molecular orbital which has primarily d_{z^2} character shown in Figure 4 is Re-O σ antibonding and Re—C≡C π antibonding.

The relative energies of some of the orbitals shown in Figure 4 can be determined from the relative polarizations in the single-crystal absorption spectra, the relative intensity changes in

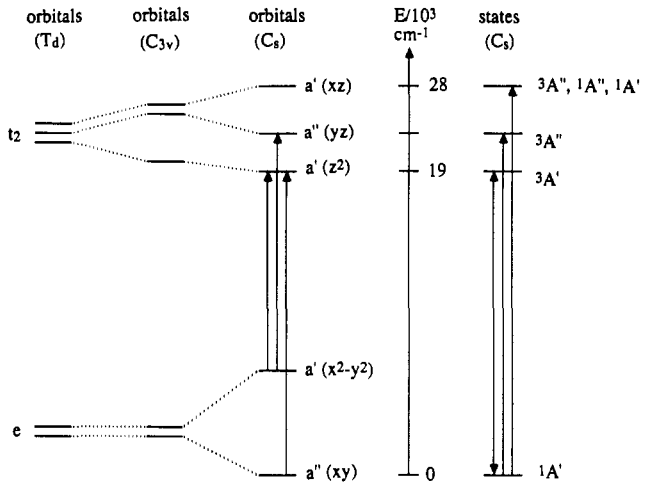

Figure 4. Molecular orbital correlation diagram (T_d, C_{3v}, and C_s point groups) and electronic states (C_s point group) for the title compounds. The observed transitions are indicated by arrows.

the resonance Raman spectra, and the results of molecular orbital calculations. From the molecular orbital calculations the LUMO is expected to be the a' orbital primarily metal d_{z^2} in character. The two occupied molecular orbitals are the a' $d_{x^2-y^2}$ and the a'' d_{xy} orbitals. The polarized spectra show that the polarization of the lowest energy absorption band is opposite to those of the next two absorption bands. Thus if the lowest energy transition is a' → a', $^1A' \rightarrow {}^3A'$, the next two transitions must be primarily $^1A' \rightarrow {}^3A''$ in order to be consistent with the observed polarizations. We assign the lowest energy band to $^1A' \rightarrow {}^3A'$ based on its molar absorptivity. The highest energy band may be a composite of $^3A''$, $^1A''$, and perhaps the $^1A'$ counterpart to the lowest excited state. The one-electron transitions corresponding to the A' → A'' transition can be a' → a'' or a'' → a'. Several d orbital orderings could give rise to these state symmetries. A choice consistent with the molecular orbital calculation is shown in Figure 4.

The resonance Raman intensities support the assignment of the lowest energy transition to the $d_{x^2-y^2}(a') \rightarrow d_{z^2}(a')$ orbitals. The intensity of a band in a resonance Raman spectrum is related to the magnitude of the bond length change between the atoms involved in that normal mode.[13-15] The spectrum taken with the exciting light in resonance with the lowest energy excited state shows significant enhancement of the Re–O stretching mode, consistent with the population of the d_{z^2} orbital, which is strongly Re–O antibonding in character. The intensity of the Re–O stretching band observed when the excitation wavelength is in resonance with the second highest energy absorption band is much smaller, suggesting that the d_{z^2} orbital is not involved. These semiquantitative arguments support the ordering of the orbitals shown in Figure 4.

Radiative and Nonradiative Relaxation. The lifetimes of the luminescence of the complexes studied here (10 μs) are typical of spin-forbidden d–d transitions in third-row transition-metal complexes. The observed lifetimes for the three complexes are similar at 20 K, the lowest temperature studied. As the temperature is raised the lifetimes decrease (Figure 2). The curves for the two methylacetylene complexes are roughly parallel while that for the phenylacetylene complex decreases much more rapidly. The radiative lifetimes for the complexes are calculated to be on the order of 60 μs based on the oscillator strengths of the $^1A' \rightarrow {}^3A'$ absorption band.[16] The observed lifetimes (10–20 μs) are shorter and suggest that nonradiative mechanisms are important. Two different nonradiative relaxation mechanisms are compared to the experimental findings in the following discussion.

Intramolecular multiphonon relaxation processes are known to be efficient in many different metal complexes. The nonradiative relaxation rate increases with the increasing number of high-energy oscillators around the metal center, leading to a decrease of both the luminescence lifetime and the intensity.[17-20] If the C—H oscillators in the title compounds are counted, the following ordering of the luminescence lifetimes is expected: $[Re(O)PPh_3(CH_3C{\equiv}CCH_3)_2]SbF_6$ (27 C—H oscillators) shorter than $Re(O)I(C_6H_5C{\equiv}CC_6H_5)_2$ (20 C—H) shorter than $Re(O)I(CH_3C{\equiv}CCH_3)_2$ (12 C—H). This simple order is in agreement with the experimental data in Figure 2, indicating that intramolecular multiphonon processes provide the dominant relaxation pathway.

Intermolecular energy-transfer processes to impurities or lattice defects provide a different relaxation pathway. Evidence for the existence of these processes is provided by the slight difference in the temperature dependence of the lifetime compared to that of the luminescence intensity shown in Figure 2 for each of the title compounds. However, the luminescence behavior is dominated by intramolecular multiphonon relaxation processes.

Conclusions

The lowest energy excited state of the title compounds arises from a $d_{x^2-y^2} \rightarrow d_{z^2}$ transition. The assignment is supported by the relative polarization in the absorption spectra, the resonance enhancement in resonance Raman spectra, and previously reported molecular orbital calculations. The temperature dependence of the luminescence lifetimes and intensities correlate with the number of high-frequency C–H modes, suggesting that intramolecular nonradiative relaxation is the dominant relaxation mechanism.

Acknowledgment. This work was made possible by a grant from the National Science Foundation (CHE88-06775). We thank Professor J. Mayer for the gift of the compounds used in this study.

(13) Heller, E. J. *Acc. Chem. Res.* **1981**, *14*, 368.
(14) Zink, J. I. *Coord. Chem. Rev.* **1985**, *64*, 93.
(15) Shin, K.-S. K.; Zink, J. I. *Inorg. Chem.* **1989**, *28*, 4358.
(16) Imbusch G. F.; Kopelman, R. In *Laser Spectroscopy of Solids*, Yen, W. M., Selzer, P. M., Eds.; Topics in Applied Physics 49; Springer Verlag: Berlin, 1981.
(17) Kühn, K.; Wasgestian, F.; Kupka, H. *J. Phys. Chem.* **1981**, *85*, 665.
(18) Petersen, J. D.; Ford, P. C. *J. Phys. Chem.* **1974**, *78*, 1144.
(19) Bergkamp, M. A.; Brannon, J.; Magde, D.; Watts, R. J.; Ford, P. C. *J. Am. Chem. Soc.* **1979**, *101*, 4549.
(20) Reber, C.; Güdel, H. U.; Buijs, M.; Wieghardt, K.; Chaudhuri, P. *Inorg. Chem.* **1988**, *27*, 2115.